

Finite Element Analysis of Low-Velocity Impact Damage on Stiffened Composite Panels

Xuan Sun, Mingbo Tong

Abstract—To understand the factors which affect impact damage on composite structures, particularly the effects of impact position and ribs. In this paper, a finite element model (FEM) of low-velocity impact damage on the composite structure was established via the nonlinear finite element method, combined with the user-defined materials subroutine (VUMAT) of the ABAQUS software. The structural elements chosen for the investigation comprised a series of stiffened composite panels, representative of real aircraft structure. By impacting the panels at different positions relative to the ribs, the effect of relative position of ribs was found out. Then the simulation results and the experiments data were compared. Finally, the factors which affect impact damage on the structures were discussed. The paper was helpful for the design of stiffened composite structures.

Keywords—Stiffened, Low-velocity, Impact, Abaqus, Impact Energy.

I. INTRODUCTION

IN order to develop a structure which are more damage-tolerant, it is necessary to understand how the damage is caused and how it affect residual performance. Many investigations of impact damage in carbon-fiber composites are usually testing on small laminates rather than full-scale structures. Several important issues regarding simulation of composite structure due to low-velocity impact were investigated including damage initiation and the corresponding change of stiffness. The analysis yields analytic functions describing the history of contact force, displacements of the impactor and the panel in three main directions. The effects of physical and geometrical parameters such as initial potential energy of the impactor, location of the impacted site on the stiffened composite panels and the material density of the core on dynamic response of stiffened composite panels have been discussed [1].

Xuan Sun is with the Key Laboratory of Fundamental Science for National-Advanced Design Technology of Flight Vehicle. Nanjing University of Aeronautics and Astronautics. Nanjing 210016, P.R.China (phone: +8615850794614; e-mail: 359188335@qq.com).

Professor Mingbo Tong is with the Key Laboratory of Fundamental Science for National-Advanced Design Technology of Flight Vehicle. Nanjing University of Aeronautics and Astronautics. Nanjing 210016, P.R.China (phone: +8613951745384; e-mail: tongw@nuaa.edu.cn).

II. FAILURE CRITERION, MATERIALS AND METHODS

A. Failure Criterion

We used the following failure criterion:

1. Fiber Direction [2]

When:

$$\sigma_{xx} \geq 0 \quad (1)$$

$$F_{XT} = \left(\frac{\sigma_{xx}}{X_T} \right)^2 + \left(\frac{\sigma_{xy}}{S_{12}} \right)^2 \quad (2)$$

or:

$$\sigma_{xx} < 0 \quad (3)$$

$$F_{XC} = \left(\frac{-\sigma_{xx}}{X_C} \right)^2 \quad (4)$$

2. Matrix Direction [3]

When:

$$\sigma_{yy} \geq 0 \quad (5)$$

$$F_{YT} = \left(\frac{\sigma_{yy}}{Y_T} \right)^2 + \left(\frac{\sigma_{xy}}{S_{12}} \right)^2 \quad (6)$$

or:

$$\sigma_{yy} < 0 \quad (7)$$

$$F_{YC} = \left(\frac{\sigma_{yy}}{2S_{23}} \right)^2 + \left[\left(\frac{Y_C}{2S_{23}} \right)^2 - 1 \right] \left(\frac{\sigma_{xy}}{Y_C} \right) + \left(\frac{\sigma_{xy}}{S_{12}} \right)^2 \quad (8)$$

3. Delamination Direction [4]

When:

$$\sigma_{zz} \geq 0 \quad (9)$$

$$F_{ZT} = \left(\frac{\sigma_{zz}}{Z_T} \right)^2 + \left(\frac{\sigma_{yz}}{S_{23}} \right)^2 + \left(\frac{\sigma_{xz}}{S_{13}} \right)^2 \quad (10)$$

or:

$$\sigma_{zz} < 0 \quad (11)$$

$$F_{ZC} = \left(\frac{\sigma_{zz}}{Z_C} \right)^2 + \left(\frac{\sigma_{yz}}{S_{23}} \right)^2 + \left(\frac{\sigma_{xz}}{S_{13}} \right)^2 \quad (12)$$

B. Materials and Lay-UPS

For 15 J impacts, the geometrical parameters for the stiffened composite panels and I-section stringers stiffened composite panel lay-ups see Figs. 1 and 2.

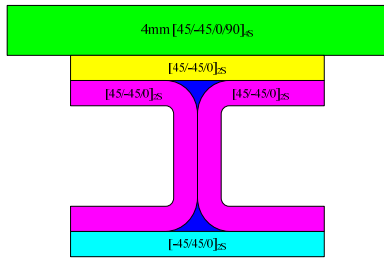


Fig. 1 Lay-ups of I-section stringers stiffened composite panel

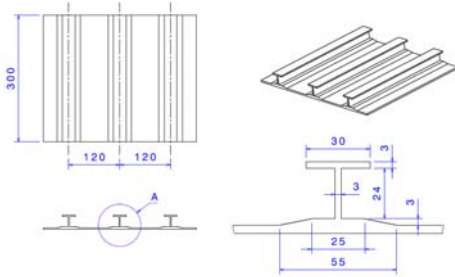


Fig. 2 Geometry of I-section stringers stiffened composite panel

The thickness of skin was 4 mm and the space between stringers was 120 mm apart. It was manufactured from Ciba T800/924. The panel skins were laid up with (+45/-45/0/90)4s lay-ups for the 4mm thick skins. The I-section stringers were assembled from four uncured laminates, comprising a tapered foot, two C-sections back-to-back and a spar cap. The foot and the C-sections had the same lay-up (+45/-45/0)2s, while that of the spar cap was (-45/+45/0). The triangular spaces between the webs and the spars were filled with strips of unidirectional prepreg. The foot and cap of each stringer had balanced lay-ups, but, as a consequence of forming two laminates into C-sections, the web was unbalanced [5], [6].

The performance parameters were shown below.

TABLE I PERFORMANCE PARAMETERS	
performance parameter	value
E11	160GPa
E22	9.2 GPa
E33	9.2 GPa
G12	6.2 GPa
G13	6.2GPa
G23	3.7 GPa
v12	0.35
v13	0.35
v23	0.4
X T	1890 MPa
X C	1615 MPa
Y T	50 MPa
Y C	250 MPa
Z T	50 MPa
Z C	250 MPa
S12	105 MPa
S13	105 MPa
S23	105 MPa

C. Methods

From preliminary studies on plain laminates, a 15 J impact; the highest unreported threat during maintenance to a military aircraft was found to produce a damage size of about 45 mm across. This energy was used to impact the skin-stringer panels at different locations (Fig. 3): (site A) over the center of a bay; (site B) over a bay, 38 mm from a stringer centerline; and (site D) directly over the centerline of a stringer [7].

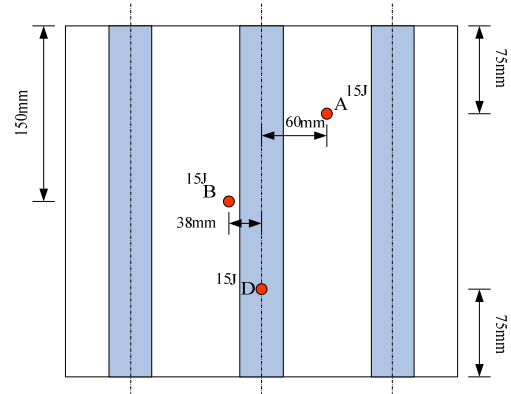


Fig. 3 Impacting sites

III. RESULTS

A. Site A

The peak force of simulation value is 6590N, and the experiment value is 6157N, so the error is 7%.

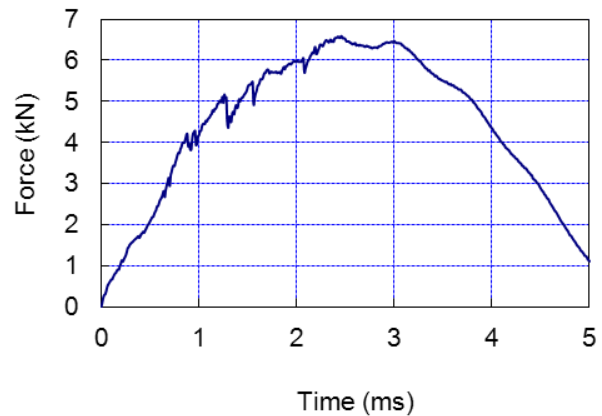


Fig. 4 Peak force on site A

The damage area is 998 mm^2 , and it is 20% smaller than experiment value.

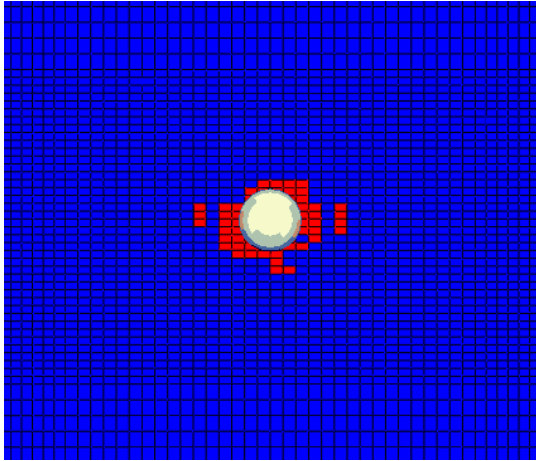


Fig. 5 Damage area on site A from top view

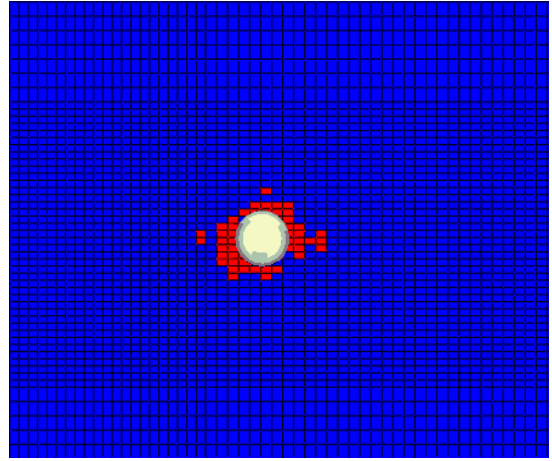


Fig. 8 Damage area on site B from top view

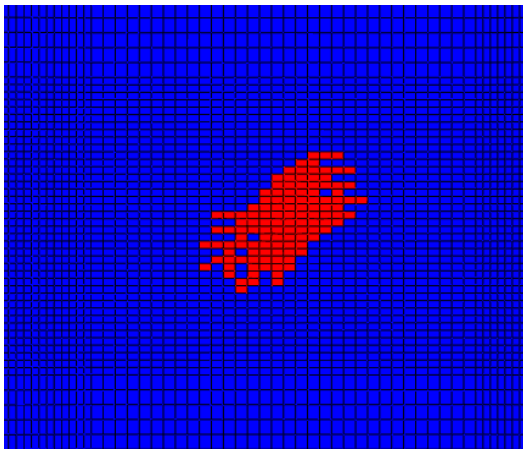


Fig. 6 Damage area on site A from bottom view

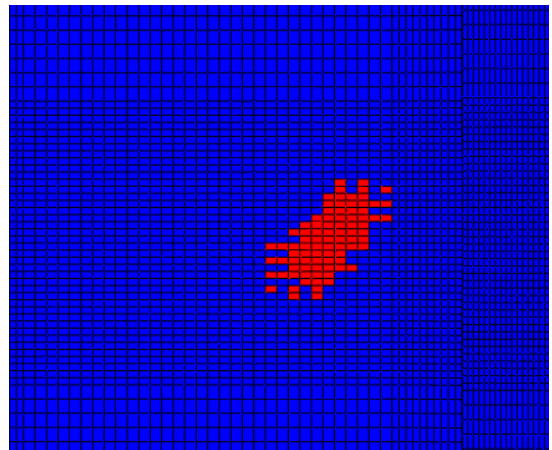


Fig. 9 Damage area on site B from bottom view

B. Site B

The peak force of simulation value is 6918N, and the experiment value is 6687N, so the error is 3.4%.

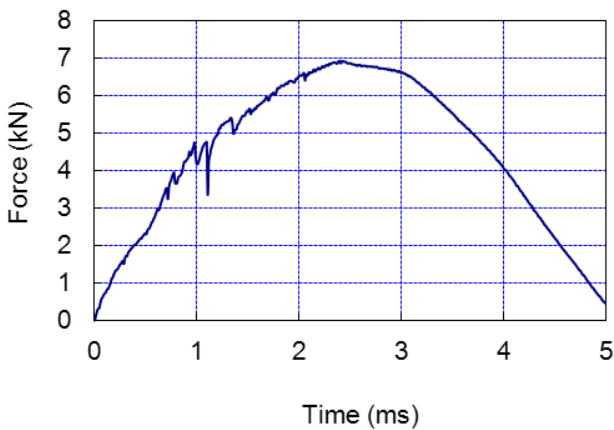


Fig. 7 Peak force on site B

The damage area is 678 mm^2 , and it is 18% smaller than experiment value .

C. Site D

The peak force of simulation value is 10768N, and the experiment value is 10425N, so the error is 3%.

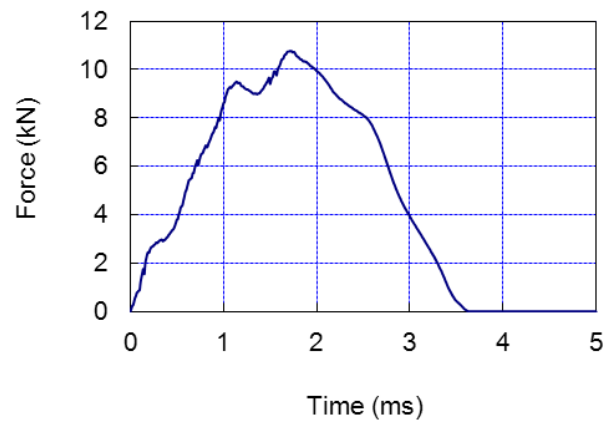


Fig. 10 Peak force on site D

The damage area is 38 mm^2 , and it is 5% smaller than experiment value .

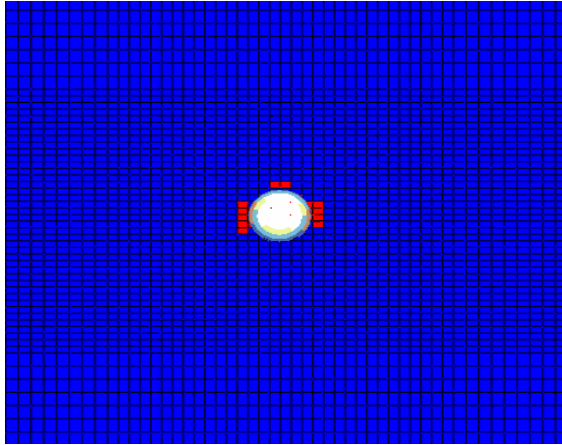


Fig. 11 Damage area on site D from top view

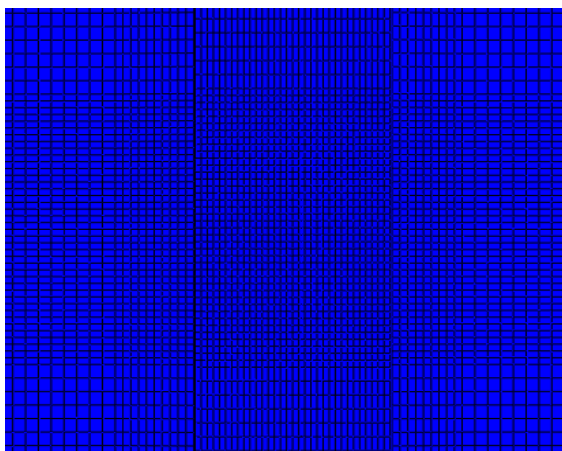


Fig. 12 Damage area on site D from bottom view

After that, we compare the result on three Sites (A,B,D).

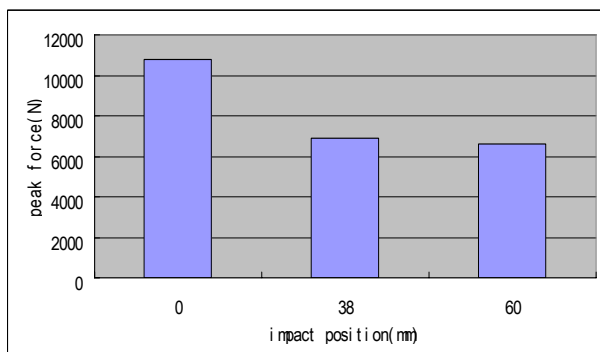


Fig. 13 Peak force on the three impact sites

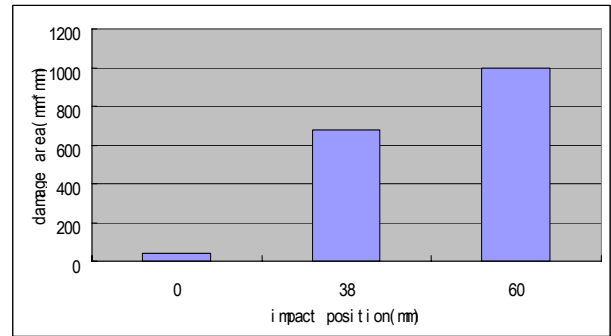


Fig. 14 Damage area on the three impact sites

The energy transmitted through elastic deformation is obviously and cause the impactor to rebound. There are three damage mechanisms occurred; matrix cracking, delamination, and fiber broken. Matrix cracking is the first damage mechanisms to occur. Delamination is the most concern in low-velocity impact, for although this damage not visible by eye, it can cause a significant reduction in the compressive.

The locations of the impacts were in centre bay between the stringers, in a bay close to a stringer, and above the stringer centreline. From Figs. 13 and 14, we can figure out that the more it is apart from stringer, the less peak force is; the more it is apart from stringer, the more damage area is. For impacts in the bay, a compliant bay led to increased absorption of the incident energy through elastic structural response. However, for impacts in the foot, a compliant bay led to increased absorption of the incident energy through damage to the substructure. For impacts over the stringer centreline, much of the incident energy was absorbed through elastic deformation of the substructure. So the result in my paper is acceptable.

IV. DISCUSSION

The proximity of substructure would significantly affect energy absorption and damage mechanism. They depend on the complex interaction of these structural details. It is necessary to understand the way how the structure influences damage. When impacting happened, the kinetic energy of the impacting should be transmitted to structure, fully or partly. These may be elastic deformation of structure, vibration of structure and damage of structure. The impactor rebound because that the energy transmitted through elastic deformation is recoverable, but the damage can't recover. It includes three types of damage mechanisms: fibre broken, matrix cracking, delamination.

The first damage type occurred is matrix cracking. Delamination is most concerned damage type in low-velocity impact. Although it is not visible, it also can cause a significant reduction in CAI (compressive after impact).

Because of complicated damage type, the damage extent is not exactly reflecting the degree of damage, so the residual strength is not directly related to the impact damage size.

V. CONCLUSIONS

We did this job to identify delamination shape and position. The locations of impact were with respect to stringer: In bay

close to stringer, in bay between the stringer and on the stringer centreline.

The test result of impact on plain laminates can't be applied to structures.

The structure geometry decided the structure's damage resistance. The incident energy was absorbed mainly through elastic of structure when impact in the bay. However, it was absorbed through damage of stringer when impact on the substructure.

When impact in the bay, the delamination shape was almost circular. However, when impact near the stringer, the delamination shape became elliptical, sometimes peanut shape. We can figure out that during impact, delamination tended to grow towards regions of different stiffness.

The type and distribution of damage changed where the skin attached to stringer. The delamination became larger towards the back side in the bay, however, the delamination was mainly near the front face and fiber broken happened.

ACKNOWLEDGMENT

We wish to acknowledge the COMAC (Commercial Aircraft Corporation of China Ltd) for the conditions and resources.

REFERENCES

- [1] E. Greenhalgh, S. M. Bishop, Characterisation of impact damage in skin-stringer composite structures. Elsevier Science Ltd. Composite Structures 36 (1996) 187-207.
- [2] A.N. Palazotto, Finite element analysis of low-velocity impact on composite sandwich plates. Elsevier Science Ltd. Composite Structures 49 (2000) 209±227.
- [3] Joshi S P, Sun C T. Impact induced fracture in a laminated composite [J]. J. Comps. Mater., 1985, 19: 51-66.
- [4] Choi H Y, Chang F K. A model for predicting damage in graphite / epoxy laminate composites resulting from low velocity point impact [J]. J. Compos. Mater. , 1992, 26: 2134-69.
- [5] Chang F.K., Lessard L.B. Damage Tolerance of Laminated Composites Containing an Open Hole and Subjected to Compressive Loadings: I-Analysis. Journal of Composite Materials. 1991, 25(1):2-43.
- [6] Maimia P., Camanhob P.P., Mayugoa J.A., et al. A continuum damage model for composite laminates: Part I - Constitutive model. Mechanics of Materials. 2007, 39(10):897-908.
- [7] Soutis C., Fleck N.A. Static Compression Failure of Carbon Fibre T800/924C Composite Plate with a Single Hole. Journal of Composite Materials. 1990, 24:536-558.



Xuan Sun was born in Hangzhou China. He is currently a final year doctoral candidate at Nanjing University of Aeronautics and Astronautics, in the Key Laboratory of Fundamental Science for National-Advanced Design Technology of Flight Vehicle.

Xuan Sun research interests involve composite structure and crashworthiness.



Mingbo Tong was born in Leshan China. He is professor at Nanjing University of Aeronautics and Astronautics, in the Key Laboratory of Fundamental Science for National-Advanced Design Technology of Flight Vehicle. He is the college principal.

Mingbo Tong research interests involve composite structure, crashworthiness, CFD and metal structure.